Ecto-F1-ATPase and MHC Class I Close Association on cell membranes.

Pierre Vantourout, Laurent O. Martinez, Aurélie C.S. Fabre, Xavier Collet, Eric Champagne

Title

Ecto-F_1-ATPase and MHC Class I Close Association on cell membranes

Authors

Pierre Vantourout[1,2], Laurent O. Martinez[1,2], Aurélie Fabre[1,2], Xavier Collet[1,2] and Eric Champagne[1,2,3].

Affiliations :

[1]INSERM, U563, Centre de Physiopathologie de Toulouse Purpan, Département Lipoprotéines et Médiateurs Lipidiques, Toulouse, F-31000, France.
[2]Université Toulouse III Paul Sabatier, Institut Claude de Préval (IFR30), Toulouse, F-31000, France ;
[3]corresponding author

Correspondence / Reprint request

Eric Champagne, INSERM U563, Bâtiment C, CHU Purpan, BP3028, F-31024, Toulouse, France.
Phone : (33) 5 61 15 84 33
Fax : (33) 5 61 15 84 28
E.mail : Eric.Champagne@toulouse.inserm.fr

Mailing address for all authors:

Centre de Physiopathologie de Toulouse Purpan, INSERM U563, Département LML, CHU Purpan, BP3028, Toulouse, F-31024, France.

ABSTRACT

Subunits of the mitochondrial ATP synthase complex are expressed on the surface of tumors, bind the TCR of human Vγ9/Vδ2 lymphocytes and promote their cytotoxicity. Present experiments show that detection of the complex (called ecto-F_1-ATPase) at the cell surface by immunofluorescence correlates with low MHC-class I antigen expression. Strikingly, the α and β chains of ecto-F_1-ATPase are detected in membrane protein precipitates from immunofluorescence-negative cells, suggesting that ATPase epitopes are masked. Removal of β2-microglobulin by mild acid treatment so that most surface MHC-I molecules become free heavy chains reveals F_1-ATPase epitopes on MHC-I^+ cell lines. Ecto-F_1-ATPase is detected by immunofluorescence on primary fibroblasts which express moderate levels of MHC-I antigens. Upregulation of MHC-I on these cells following IFN-γ and/or TNF-α treatment induces a dose-dependent disappearance of F_1-ATPase epitopes. Finally, biotinylated F_1-ATPase cell surface components co-immunoprecipitate with MHC-I molecules confirming the association of both complexes on Raji cells. Confocal microscopy analysis of MHC-I and ecto-F_1-ATPase β chain expression on HepG2 cells shows a co-localization of both complexes in punctate membrane domains. This demonstrates that the TCR target F_1-ATPase is in close contact with MHC-I antigens which are known to control Vγ9/Vδ2 T cell activity through binding to natural killer inhibitory receptors.

Keywords:
Innate immunity, Gamma-delta lymphocytes, ATP synthase, MHC Class I antigens

Non-standard abbreviations:

ApoA1: apolipoprotein A-I
β2m: beta-2-microglobulin
α-F_1, β-F_1: alpha and beta subunits of F_1 domain of ATP synthase
EBV-B: Epstein Barr Virus-immortalized B cell line
TAP: transporter associated with antigen processing
MHC-I: MHC class I antigens
iNKR: inhibitory natural killer cell receptor for MHC class I antigens

1. Introduction

T lymphocytes expressing an antigen receptor (TCR) of the γδ type represent a small fraction (1-5%) of T cells in human blood and lymph nodes although they may be more abundant in mucosae-associated lymphoid tissues. Striking features of these lymphocytes include an activated cell phenotype and a biased TCR V gene repertoire varying with their tissue distribution, so that the vast majority of human peripheral γδ cells express a Vγ9/Vδ2 TCR variable region gene combination (see (Hayday, 2000; Pennington et al., 2005) for reviews). These Vγ9/Vδ2 T cells proliferate in vivo and in vitro in response to bacterial non-peptidic phosphorylated antigens termed phosphoantigens (PAg) in a TCR-dependent manner. To date the most powerful natural phosphoantigen is hydroxy-dimethylallyl pyrophosphate (HDMAPP), a metabolite of the 1-deoxy-D-xylulose-5-phosphate (DOXP) pathway of isoprenoid biosynthesis in plants and bacteria. (Bukowski et al., 1998; Morita et al., 2007; Poupot and Fournie, 2004). How the bacterial PAgs produced by infected cells are presented to T cells is poorly understood although evidence exist that this requires a cell-cell contact which can be between sister Vγ9/Vδ2 T cells (Bonneville and Fournie, 2005; Green et al., 2004; Lang et al., 1995; Morita et al., 1995).

Vγ9/Vδ2 T cells are also activated by several tumoral cell lines including hematopoietic tumors Daudi (Burkitt's lymphoma), RPMI8226 (myeloma) and K562 (erythroleukemia), and solid tumors such as renal cell carcinomas which are frequently found to be associated with Vγ9/Vδ2 T cell infiltrates in vivo (Zocchi and Poggi, 2004). Recent findings implicate ubiquitous endogenous phosphoantigens (isopentenyl pyrophosphate and dimethylallyl-pyrophosphate) in Vγ9/Vδ2 T cell activation by tumors. Indeed, their accumulation or depletion following modulation of the mevalonate pathway by aminobisphosphonates or statins leads to an increase or decrease of the stimulatory activity, respectively (Gober et al., 2003). Again, activation by these metabolites is likely to require some form of antigen presentation by unknown structures.

We recently described the presence of components of the mitochondrial ATP synthase on the surface of tumor cells with stimulatory activity for Vγ9/Vδ2 lymphocytes (Scotet et al., 2005). This structure, referred to as ecto-F_1-ATPase (F_1) binds a soluble form of Apolipoprotein A-I (ApoA1) so that an F_1-ApoA1 complex is frequently detected on the surface of stimulatory tumors. Moreover, purified soluble forms of F_1 and ApoA1 both specifically bind to a recombinant soluble Vγ9/Vδ2 TCR and the F_1-ApoA1 complex is stimulatory for Vγ9/Vδ2 T cells when immobilized on polystyrene beads. These components could be involved in endogenous phosphoantigen presentation although there is still no direct evidence for this.

Cell surface expression of F_1 is not confined to tumor cells as several studies have shown the presence and enzymatic activity of F_1 on hepatocytes, keratinocytes or endothelial cells (Burrell et al., 2005; Champagne et al., 2006; Martinez et al., 2003; Moser et al., 1999). In the present paper, we provide evidence that F_1 is more frequently expressed on the surface of tumoral and non tumoral cells than previously thought on the basis of immunofluorescence analyses and that a close association exists between F_1 and Major Histocompatibility Complex class I antigens (MHC-I). Indeed, when these antigens are highly expressed, they can prevent F_1 detection. Knowing that Vγ9/Vδ2 T cell activation is strictly controlled by activatory and inhibitory receptors for MHC-I antigens (Fisch et al., 1997; Halary et al., 1997; Poccia et al., 1997; Trichet et al., 2006), this has important functional implications regarding the regulation of their antitumoral and inherent anti-self reactivity.

2. Material and methods

2.1. Tumor cell lines, cultures and antibodies

Cell lines are from the ATCC except the human β2m Daudi transfectant (Anne Quillet, Toulouse, France) and RCC7 (Anne Caignard, Villejuif, France). 721.221 (MHC-I deficient (Shimizu and De Mars, 1989)) and Awells (IHW#9090) are EBV-B cell lines. ST-EMO (EBV-B) and ST-F1 (primary fibroblast) are derived from a TAP-deficient patient (provided by Henry de la Salle, Strasbourg, France). HD-F1 are normal primary foreskin fibroblasts obtained from Purpan Hospital pediatric surgery department (Toulouse, France). RMA is a murine T lymphoma and RMA-S is its TAP-deficient variant (Ljunggren and Karre, 1985). Cell lines were cultivated in RPMI 1640 medium except for HepG2, primary fibroblasts and RCC7 (DMEM), supplemented with FCS, glutamine and antibiotics.

The monoclonal anti-α (clone 7H10, IgG_{2b}) and anti-β (clone 3D5, IgG_1) F_1-ATPase antibodies used for immunofluorescence were from Molecular Probes. For immunoblotting studies, anti-α-F_1 (clone 51, IgG2a) and anti-β-F_1 (clone 10, IgG_1) were from BD Biosciences. The anti-cytochrome c antibody (clone 7H8.2C12, IgG_{2b}) was from R&D Systems. The anti-HLA-DR FITC antibody (Immu-257, IgG_1) and isotype controls were from Beckman-Coulter. The anti-CD19 antibody (clone LT19, IgG_1) was from Exbio (Prague, Czech Republic). The HC10 (anti-MHC-I free heavy chain) antibody (Stam et al., 1990) was kindly provided by Dr H.L Ploegh (Cambridge, MA). The W6/32 hybridoma (anti-HLA-class I) was obtained from ATCC. The anti-H-$2K^bD^b$ was from Cedarlane Laboratories.

2.2. Induction of MHC-I expression by cytokines and flow cytometry analysis

Fibroblast cells and other adherent cell lines were plated the day before treatment on 6-well dishes. Control Daudi cells were grown in suspension. For MHC class-I induction experiments, IFN-γ and/or TNF-α (Biosource) were added to cell cultures (48h). Adherent cells were harvested using ice-cold PBS containing 10mM EDTA. Cells were then washed with PBS 5% FCS (FACS medium). Staining and washing were performed in FACS medium using a standard indirect immunofluorescence procedure. Primary mAbs and isotypic controls were used at the concentration of 5-10µg/ml. Secondary staining was performed using polyclonal goat $F(ab)'_2$ anti-mouse IgG-FITC (Dako Cytomation). Data were acquired on a FACScan flow cytometer (BD Biosciences).

2.3. Disruption of cell surface MHC-I by acid treatment

The procedure described by Dong *et al*. was used (Dong et al., 2003) with minor modifications. Briefly, cells were harvested, washed once in PBS and incubated for 1min on ice in 1ml of citrate-phosphate buffer (66mM NaH_2PO_4, 131mM citric acid, 1% BSA, pH 3) or PBS as a control. pH was neutralized by the addition of 9ml of PBS (pH 13), and cells were pelleted, washed once with FACS medium, and stained immediately for flow cytometry analysis or put back in culture.

2.4. Streptavidin pull-down and co-immunoprecipitation experiments

Biotinylation and precipitation of cell surface proteins was performed according to Altin *et al* (Altin and Pagler, 1995) with few modifications using the membrane-impermeant NHS-LC-biotin reagent (Pierce, 0.25mg/ml). Co-precipitation of F_1 components with MHC did not require cross-linking. After cell lysis (150mM NaCl, 1% Triton X-100, Tris 20mM, pH7.6, anti-proteases) and centrifugation (10000g, 15min, 4°C) to remove insoluble material, lysates were pre-cleared with CL4B-sepharose beads and incubated for 3h at 4°C with streptavidin-sepharose beads (GE Healthcare) or with protein G-sepharose beads previously incubated with mAbs (1µg). Proteins were eluted at 100°C in Laemmli buffer (5% 2-ME) and loaded for standard 12% SDS-PAGE and transferred to nitrocellulose. Immunodetection was performed using primary antibodies at 1µg/ml followed by a secondary goat anti-mouse IgG-

Horse Radish Peroxidase-conjugated Ab (Mouse Trueblot, eBioscience, SanDiego, CA) or streptavidin-HRP (GE Healthcare) and chemiluminescence (Sigma Co.).

2.5. Confocal microscopy

HepG2 cells were seeded (10^6 cells/well, 48h) on collagen-I-coated round coverslips (Biocoat, BD Biosciences) in 6-wells culture plates. Cells were then washed and fixed (4% paraformaldehyde, 15min, 4°C) and coverslips were saturated (PBS plus 0.2% gelatin, 1h, room temperature). After addition of primary mAb (3D5, anti-βF_1, IgG_1, 10µg/ml, 1hr, 4°C), samples were washed and stained with Alexa 568-conjugated anti-IgG_1 (Molecular Probes) and FITC-conjugated W6/32 mAb (IgG_{2a}). After washing, coverslips were dried, mounted on slides (PBS, 90% glycerol, 2.5% DABCO) and examined using a LSM510 confocal microscope (Carl Zeiss). The absence of cross-reactivity of anti-IgG1 antibodies towards IgG2a was checked.

3. Results

3.1. Ecto-F_1-ATPase and MHC-I expression by cytometry

We previously documented the expression of components of F_1 on the surface of cell lines sensitive to lysis by Vγ9/Vδ2 lymphocytes. Other studies have independently reported the presence of the same components on hepatocytes (Martinez et al., 2003), endothelial cells (Chang et al., 2002; Moser et al., 1999), adipocytes (Kim et al., 2004) or keratinocytes (Burrell et al., 2005). We have now extended these findings by the cytofluorometry analysis of several other tumoral and non tumoral cell lines (Fig.1). In addition to Daudi and K562, renal carcinomas and HepG2 tumors, the α and β subunits of F_1 are readily detected on the surface of HeLa cells and primary fibroblasts. As previously reported, these components are very weakly or not detected on Raji cells, Jurkat cells, and most EBV-transformed B-lymphoblastoid cells lines such as Awells, LG2, RPMI-8866 (Fig.1 and data not shown). Daudi cells barely express MHC class-I antigens due to the lack of the MHC-I light chain β2-microglobulin (β2m). Strikingly F_1 is undetectable on β2m-transfected Daudi cells which express high levels of MHC-I. F_1 is also detected on the TAP-deficient B-lymphoblastoid line ST-EMO which has a strongly reduced expression of MHC-I antigens due to abnormal peptide loading. Similar observations can be made with the murine T cell lymphoma RMA (F_1^-) and its TAP-deficient counterpart RMA-S (F_1^+). This suggests that surface staining of F_1 components correlates with a lower level of MHC-I expression. The correlation is however not absolute since the MHC-I-deficient 721.221 B-EBV cell line does not stain for F_1.

3.2. Biochemical detection of ecto-F_1-ATPase

In order to examine the presence of ecto-F_1 components using a biochemical approach, cell surface proteins from F_1^+ and F_1^- lines were biotinylated and solubilized membrane proteins were precipitated with streptavidin, separated on a polyacrylamide gel and immunoblotted with anti-α and anti-β-F_1 antibodies (Fig.2). This confirmed the presence of the α and β-F_1 chains on the surface of Daudi and K562 cells. Strikingly, the same components were also present in the precipitates of surface proteins from cell lines staining negatively, Awells and Jurkat. As a control for a possible mitochondrial contamination of streptavidin precipitates, membranes were also immunoblotted with an anti-cytochrome c antibody. The absence of detection of cytochrome c in streptavidin precipitates indicates that mitochondrial contamination is unlikely to account for the detection of F_1 components. More likely, this suggests that F_1 is present on Jurkat and Awells cells but was not detected by flow cytometry.

3.3. MHC-I antigens mask ecto-F_1-ATPase epitopes

The inverse correlation between F_1 and MHC-I detection suggests that MHC-I expression might interfere with F_1 detection. In order to confirm this hypothesis, we took advantage of the HD-F1 primary fibroblasts which stain strongly for α and β-F_1. On this line, MHC-I antigens are expressed to a moderate level and can be strongly up-regulated in a dose dependent manner following culture in the presence of varying doses of interferon γ (IFN-γ) and tumor necrosis factor α (TNF-α). Cytokine-treated cells were thus monitored for F_1 and MHC-I expression by FACS. The experiment depicted in Figure 3 shows that the β-F_1 chain staining progressively declines while MHC-I antigens are up-regulated on the HD-F1 cell surface. Optimal treatment with the TNF-α/IFN-γ cytokine combination leads to an about 65% reduction of β-F_1 staining while MHC-I expression is stimulated ~11 folds. Interestingly, the modulation of β-F_1 staining is more sensitive to TNF-α treatment than to IFN-γ treatment. Conversely, overall MHC-I antigens are up-regulated more strongly with IFN-γ than with TNF-α, in accordance with published observations (Johnson, 2003). Similar results have been obtained using the HepG2 hepatocarcinoma line. When this cytokine treatment is applied to the MHC-I deficient lines Daudi and K562, this does not lead to significant variations of F_1 staining, indicating that the decrease in F_1 staining on fibroblasts or HepG2 cells is not due to a down modulation of β-F_1 on the cell surface following cytokine treatment (data not shown). However, these experiments do not formally exclude a coordinated inverse regulation of ecto-F_1 and MHC-I antigens.

Polakova et al. (Polakova et al., 1993) have previously shown that short acid treatment of mammalian cells at low pH promotes the dissociation of MHC-I antigens leading to the loss of antigenicity (Sugawara et al., 1987) and release of β2m so that acid-treated cells display essentially free MHC-I heavy chains. In an attempt to reveal ecto-F_1-ATPase on the surface of MHC-I-high cells, we used this approach to disrupt MHC antigens. This treatment was applied to Raji cells, which support this treatment with no visible change in morphology as evaluated by the forward and side scatter analysis by FACS, without significant cell death monitored by trypan blue incorporation, and no cell permeabilization monitored by propidium iodide staining (data not shown). MHC-I conformation was evaluated by cell staining with W6/32 antibody which detects native MHC-I antigens and HC10 which reacts selectively with free heavy chains. Acid treatment of Raji cells leads to an ~80% decrease of native MHC-I expression whereas the presence of free heavy chains is increased ~10 folds. Concomitantly, the α and β-F_1 chains are revealed on the surface of acid treated cells whereas the staining for MHC-II or CD19 antigens, used as controls, are unchanged (Fig.4a,b). Acid-treated cells are still viable and can be re-cultured. This leads to a fast re-expression of native MHC-I antigens with a full recovery at ~6h. This is accompanied by a concomitant decrease of β-F_1 staining (Fig.4c). The same acid treatment performed on MHC-deficient K562 (F_1^+) and 721.221(F_1^-) cells does not induce any significant change in F_1 subunits detection, indicating that this is not a staining artifact due to acid treatment (data not shown). As metabolic modulation of antigen expression is not possible in this experimental setting, we conclude that MHC-I dissociation reveals F_1 α and β epitopes on the surface of MHC-I-high cells. This is an indication of the close proximity of these structures on the cell surface.

3.4. Close association between ecto-F_1-ATPase components and MHC-I

In order to obtain direct evidence for an interaction between ecto-F_1 and MHC-I, we attempted to co-precipitate the complexes from lysates of MHC-I-high cells. Cells were surface-biotinylated and lysed. MHC-I antigens were immunoprecipitated using the W6/32 antibody, putative complexes were dissociated on a denaturing polyacrylamide gel and immunoblotted for the detection of F_1 components (Fig.5). Immunoprecipitation of MHC-I brings down several membrane proteins revealed by blotting with steptavidin among which

proteins at ~50kDa membrane proteins. Immunoblotting of the membrane with an anti-α-F_1 antibody allows detection of a protein which migrates as the mitochondrial α-F_1 (55 kDa) detected in total cell lysates. Similarly, immunoblotting with an anti-β-F_1 antibody reveals that the β subunit (52 kDa) is also present in the MHC-I precipitate. This is a strong indication that ecto-F_1 and MHC-I antigens can be closely associated.

Finally, the co-localization of MHC-I and ecto-F_1 was analyzed by confocal microscopy using HepG2 cells on which the moderate MHC-I expression allows the detection of both complexes (Fig.6). On these cells, β-F_1 staining reveals patch-like structures on the cell surface as already reported on other cell types (Bae et al., 2004; Kim et al., 2004). Similar patches are also revealed with the anti-MHC-I although these antigens are also present on the remaining of the plasma membrane where they are more evenly distributed. Superimposition of MHC-I and F_1 images indicates that F_1 and MHC-I antibodies effectively co-localize on the plasma membrane but, unlike MHC antigens, F_1 seems to be present selectively in the patch-like structures.

4. Discussion

In this work we provide evidence that ecto-F_1-ATPase components are present on the cell surface of several cell lines in close proximity to MHC-I antigens. This proximity is such that it prevents antibody detection of F_1 epitopes when MHC-I expression is sufficiently high. Moreover, MHC-I antigens co-precipitate with α and β-F_1 subunits. This reveals a direct contact between these structures. The first question which comes to mind is whether the size of the two complexes is compatible with these observations. Assuming that ecto-F_1 has a structural arrangement similar to that of mitochondrial F_1-ATPase, the height of the ecto-domain above the membrane would be 83 Å for the α3β3 domain plus 50 Å for the central stalk of the complex connecting the α3β3 domain to the intra-membrane F_o domain (Stock et al., 2000). The height of the extra-membrane domain of MHC-I molecules is 70 Å as determined by crystallographic analysis (Bjorkman et al., 1987). There is thus a possible 20 Å overlap between the bottom part of the α3β3 domain and the top part of the MHC-I molecule. This putative overlapping region would then correspond to the C-terminal ends of α and β-F_1. The epitopes recognized by the antibodies used in immuno-fluorescence studies are not known but it is quite possible that the putative overlapping region contains multiple antibody epitopes which can be masked by the interaction. The $(\alpha\beta)_3$ stoichiometry of the F_1 complex is compatible with the observation that the density of MHC-I molecules on the cell surface influences the number of available epitopes for antibody binding.

The tissue distribution of ecto-F_1-ATPase is not known, essentially due to the lack of antibodies able to label this structure on paraffin-embedded tissues. Many cell types have now been found to express ecto-F_1-ATPase and this raises the possibility that this complex could have a ubiquitous distribution at the surface of mammalian cells. Indeed the ecto-F_1-ATPase is detected on hepatocarcinoma cells, renal cell carcinomas, myeloma cells and Burkitt's lymphoma cells. This is not limited to tumor cells as we and others have found it expressed on primary fibroblasts (Fig.1), on primary hepatocyte cultures (Martinez et al., 2003) and HUVEC cells (Chang et al., 2002; Moser et al., 1999). All these cell types display a low or moderate level of MHC-I antigens. On Raji and Jurkat cells, the presence of F_1 is revealed by MHC-I disruption.

On most EBV-transformed lymphoblastoid cell lines, F_1 expression is undetectable by cytometry. Until now, the only exception is the TAP-deficient ST-EMO lymphoblastoid B cell line which was derived from an immunodeficient patient and clearly expresses ecto-F_1. One should notice that MHC-I expression on most EBV lines is so high that knock-down of β2m using the small interfering RNA method keep MHC-I levels above that of cells which

are spontaneously F_1^+ (data not shown). However MHC-I disruption by acid treatment of Awells cells can reveal F_1 expression (not shown) and α and β-F_1 chains can be labeled by surface biotinylation of these cells (Fig.2). This indicates that F_1 is indeed present on the surface of at least some EBV-B cells. 721.221 may represent an exception as all attempts to detect F_1 have failed in spite of extremely low MHC-I expression.

Results from Daudi (β2m-deficient), ST-EMO and RMA-S (TAP-deficient) and their $\beta2m^+$ or TAP^+ counterparts , in conjunction with the effect of β2m disruption by acid treatment suggest that MHC-I structures masking F_1 epitopes are β2m- and TAP-dependent. Immunoprecipitation experiments suggest that they are also reactive with W6/32 and thus conventional MHC-Ia antigens (HLA-A,B,C) as well as MHC-Ib HLA-G,E are good candidates. They must be weakly or not expressed on fibroblasts and more readily induced by TNF-α than by IFN-γ on these cells as opposed to overall MHC-I antigens. They most probably have a murine counterpart as deduced from F_1-masking on RMA cells. Previous studies have reported a differential IFN-γ inducibility for MHC-I loci. This is the case for HLA-B as compared to HLA-A and C (Hakem et al., 1989; Johnson, 2003) and for HLA-G as compared to HLA-B and C (Yang et al., 1996) whereas HLA-C is poorly inducible (Tibensky and Delovitch, 1990). We are currently investigating whether specific isotypes preferentially interact with F_1 and whether non-conventional MHC-Ib antigens can also be part of complexes.

The nature of MHC-class I (or MHC-Ib) antigens interacting with F_1 is particularly relevant to Vγ9/Vδ2 T cell activation mechanisms. There is multiple evidence that Vγ9/Vδ2 T cells monitor MHC-class I and MHC-class Ib levels on the surface of tumors and cells presenting phosphoantigens. This is through their expression of HLA-class I-specific inhibitory receptors (iNKR) which bind conventional MHC-I molecules as well as HLA-E and G. They also express activatory receptors (such as NKG2D) which bind stress-induced MHC-like proteins MICA/B and proteins of the RAET1 family (Bacon et al., 2004). However, as the latter are not associated to β2m, they probably do not play a role in F_1 epitope masking.

We have previously shown that the Vγ9/Vδ2 TCR binds to an F_1-ATPase/ApoA1 complex and that this recognition leads to Vγ9/Vδ2 T cell activation. The close association between the TCR ligand and the inhibitory ligand which regulates its activity may represent an important way to efficiently control TCR activity. Moreover, the TCR ligand ApoA1 is detected on tumor cells and its presence correlates with the detection of β-F_1 and low MHC class-I expression (Scotet et al., 2005). It is thus possible that soluble ApoA1 somehow competes with MHC-class I on F_1 and favors TCR binding when the MHC density is low. This may represent an important mechanism controlling Vγ9/Vδ2 T cell activation.

Acknowledgements

We thank Dr H. Ploegh for generously providing the HC10 monoclonal antibody, Dr H. de la Salle for TAP-deficient lines and Pr A. Hovnanian for normal fibroblasts. We are grateful to F. L'Faqihi and S. Allart (IFR30) for their assistance in cytometry and confocal microscopy analyses. This work was supported by the Association pour la Recherche sur le Cancer (ARC, grant #3711) and the Ligue Nationale contre le Cancer (LNCC, #RAB07002BBA).

References

Altin J. G. and Pagler E. B. (1995) A one-step procedure for biotinylation and chemical cross-linking of lymphocyte surface and intracellular membrane-associated molecules. *Anal Biochem* **224**, 382-9.

Bacon L., Eagle R. A., Meyer M., Easom N., Young N. T. and Trowsdale J. (2004) Two human ULBP/RAET1 molecules with transmembrane regions are ligands for NKG2D. *J Immunol* **173**, 1078-84.

Bae T. J., Kim M. S., Kim J. W., Kim B. W., Choo H. J., Lee J. W., Kim K. B., Lee C. S., Kim J. H., Chang S. Y., Kang C. Y., Lee S. W. and Ko Y. G. (2004) Lipid raft proteome reveals ATP synthase complex in the cell surface. *Proteomics* **4**, 3536-48.

Bjorkman P. J., Saper M. A., Samraoui B., Bennett W. S., Strominger J. L. and Wiley D. C. (1987) Structure of the human class I histocompatibility antigen, HLA-A2. *Nature* **329**, 506-12.

Bonneville M. and Fournie J. J. (2005) Sensing cell stress and transformation through Vgamma9Vdelta2 T cell-mediated recognition of the isoprenoid pathway metabolites. *Microbes Infect* **7**, 503-9.

Bukowski J. F., Morita C. T., Band H. and Brenner M. B. (1998) Crucial role of TCR gamma chain junctional region in prenyl pyrophosphate antigen recognition by gamma delta T cells. *J Immunol* **161**, 286-93.

Burrell H. E., Wlodarski B., Foster B. J., Buckley K. A., Sharpe G. R., Quayle J. M., Simpson A. W. and Gallagher J. A. (2005) Human keratinocytes release ATP and utilize three mechanisms for nucleotide interconversion at the cell surface. *J Biol Chem* **280**, 29667-76.

Champagne E., Martinez L. O., Collet X. and Barbaras R. (2006) Ecto-F1Fo ATP synthase/F1 ATPase: metabolic and immunological functions. *Curr Opin Lipidol* **17**, 279-84.

Chang S. Y., Park S. G., Kim S. and Kang C.-Y. (2002) Interaction of the C-terminal Domain of p43 and the alpha Subunit of ATP Synthase. ITS FUNCTIONAL IMPLICATION IN ENDOTHELIAL CELL PROLIFERATION. *J. Biol. Chem.* **277**, 8388-8394.

Dong Y., Lieskovska J., Kedrin D., Porcelli S., Mandelboim O. and Bushkin Y. (2003) Soluble nonclassical HLA generated by the metalloproteinase pathway. *Hum Immunol* **64**, 802-10.

Fisch P., Meuer E., Pende D., Rothenfusser S., Viale O., Kock S., Ferrone S., Fradelizi D., Klein G., Moretta L., Rammensee H. G., Boon T., Coulie P. and van der Bruggen P. (1997) Control of B cell lymphoma recognition via natural killer inhibitory receptors implies a role for human Vgamma9/Vdelta2 T cells in tumor immunity. *Eur J Immunol* **27**, 3368-79.

Gober H. J., Kistowska M., Angman L., Jeno P., Mori L. and De Libero G. (2003) Human T cell receptor gammadelta cells recognize endogenous mevalonate metabolites in tumor cells. *J Exp Med* **197**, 163-8.

Green A. E., Lissina A., Hutchinson S. L., Hewitt R. E., Temple B., James D., Boulter J. M., Price D. A. and Sewell A. K. (2004) Recognition of nonpeptide antigens by human V gamma 9V delta 2 T cells requires contact with cells of human origin. *Clin Exp Immunol* **136**, 472-82.

Hakem R., Le Bouteiller P., Barad M., Trujillo M., Mercier P., Wietzerbin J. and Lemonnier F. A. (1989) IFN-mediated differential regulation of the expression of HLA-B7 and HLA-A3 class I genes. *J Immunol* **142**, 297-305.

Halary F., Peyrat M. A., Champagne E., Lopez-Botet M., Moretta A., Moretta L., Vie H., Fournie J. J. and Bonneville M. (1997) Control of self-reactive cytotoxic T lymphocytes expressing gamma delta T cell receptors by natural killer inhibitory receptors. *Eur J Immunol* **27**, 2812-21.

Hayday A. C. (2000) [gamma][delta] cells: a right time and a right place for a conserved third way of protection. *Annu Rev Immunol* **18**, 975-1026.

Johnson D. R. (2003) Locus-specific constitutive and cytokine-induced HLA class I gene expression. *J Immunol* **170**, 1894-902.

Kim B. W., Choo H. J., Lee J. W., Kim J. H. and Ko Y. G. (2004) Extracellular ATP is generated by ATP synthase complex in adipocyte lipid rafts. *Exp Mol Med* **36**, 476-85.

Lang F., Peyrat M. A., Constant P., Davodeau F., David-Ameline J., Poquet Y., Vie H., Fournie J. J. and Bonneville M. (1995) Early activation of human V gamma 9V delta 2 T cell broad cytotoxicity and TNF production by nonpeptidic mycobacterial ligands. *J Immunol* **154**, 5986-94.

Ljunggren H. G. and Karre K. (1985) Host resistance directed selectively against H-2-deficient lymphoma variants. Analysis of the mechanism. *J Exp Med* **162**, 1745-59.

Martinez L. O., Jacquet S., Esteve J. P., Rolland C., Cabezon E., Champagne E., Pineau T., Georgeaud V., Walker J. E., Terce F., Collet X., Perret B. and Barbaras R. (2003) Ectopic beta-chain of ATP synthase is an apolipoprotein A-I receptor in hepatic HDL endocytosis. *Nature* **421**, 75-9.

Morita C. T., Beckman E. M., Bukowski J. F., Tanaka Y., Band H., Bloom B. R., Golan D. E. and Brenner M. B. (1995) Direct presentation of nonpeptide prenyl pyrophosphate antigens to human gamma delta T cells. *Immunity* **3**, 495-507.

Morita C. T., Jin C., Sarikonda G. and Wang H. (2007) Nonpeptide antigens, presentation mechanisms, and immunological memory of human Vgamma2Vdelta2 T cells: discriminating friend from foe through the recognition of prenyl pyrophosphate antigens. *Immunol Rev* **215**, 59-76.

Moser T. L., Stack M. S., Asplin I., Enghild J. J., Hojrup P., Everitt L., Hubchak S., Schnaper H. W. and Pizzo S. V. (1999) Angiostatin binds ATP synthase on the surface of human endothelial cells. *Proc Natl Acad Sci U S A* **96**, 2811-6.

Pennington D. J., Vermijlen D., Wise E. L., Clarke S. L., Tigelaar R. E. and Hayday A. C. (2005) The integration of conventional and unconventional T cells that characterizes cell-mediated responses. *Adv Immunol* **87**, 27-59.

Poccia F., Cipriani B., Vendetti S., Colizzi V., Poquet Y., Battistini L., Lopez-Botet M., Fournie J. J. and Gougeon M. L. (1997) CD94/NKG2 inhibitory receptor complex modulates both anti-viral and anti-tumoral responses of polyclonal phosphoantigen-reactive V gamma 9V delta 2 T lymphocytes. *J Immunol* **159**, 6009-17.

Polakova K., Karpatova M. and Russ G. (1993) Dissociation of beta 2-microglobulin is responsible for selective reduction of HLA class I antigenicity following acid treatment of cells. *Mol Immunol* **30**, 1223-30.

Poupot M. and Fournie J. J. (2004) Non-peptide antigens activating human Vgamma9/Vdelta2 T lymphocytes. *Immunol Lett* **95**, 129-38.

Scotet E., Martinez L. O., Grant E., Barbaras R., Jeno P., Guiraud M., Monsarrat B., Saulquin X., Maillet S., Esteve J. P., Lopez F., Perret B., Collet X., Bonneville M. and Champagne E. (2005) Tumor Recognition following Vgamma9Vdelta2 T Cell Receptor Interactions with a Surface F1-ATPase-Related Structure and Apolipoprotein A-I. *Immunity* **22**, 71-80.

Shimizu Y. and De Mars R. (1989) Production of human cells expressing individual transferred HLA-A,-B,-C genes using an HLA-A,-B,-C null human cell line. *J Immunol* **142**, 3320-8.

Stam N. J., Vroom T. M., Peters P. J., Pastoors E. B. and Ploegh H. L. (1990) HLA-A- and HLA-B-specific monoclonal antibodies reactive with free heavy chains in western blots, in formalin-fixed, paraffin-embedded tissue sections and in cryo-immuno-electron microscopy. *Int Immunol* **2**, 113-25.

Stock D., Gibbons C., Arechaga I., Leslie A. G. and Walker J. E. (2000) The rotary mechanism of ATP synthase. *Curr Opin Struct Biol* **10**, 672-9.

Sugawara S., Abo T. and Kumagai K. (1987) A simple method to eliminate the antigenicity of surface class I MHC molecules from the membrane of viable cells by acid treatment at pH 3. *J Immunol Methods* **100**, 83-90.

Tibensky D. and Delovitch T. L. (1990) Promoter region of HLA-C genes: regulatory elements common to and different from those of HLA-A and HLA-B genes. *Immunogenetics* **32**, 210-3.

Trichet V., Benezech C., Dousset C., Gesnel M. C., Bonneville M. and Breathnach R. (2006) Complex Interplay of Activating and Inhibitory Signals Received by Vgamma9Vdelta2 T Cells Revealed by Target Cell beta2-Microglobulin Knockdown. *J Immunol* **177**, 6129-6136.

Yang Y., Chu W., Geraghty D. E. and Hunt J. S. (1996) Expression of HLA-G in human mononuclear phagocytes and selective induction by IFN-gamma. *J Immunol* **156**, 4224-31.

Zocchi M. R. and Poggi A. (2004) Role of gammadelta T lymphocytes in tumor defense. *Front Biosci* **9**, 2588-604.

Figures

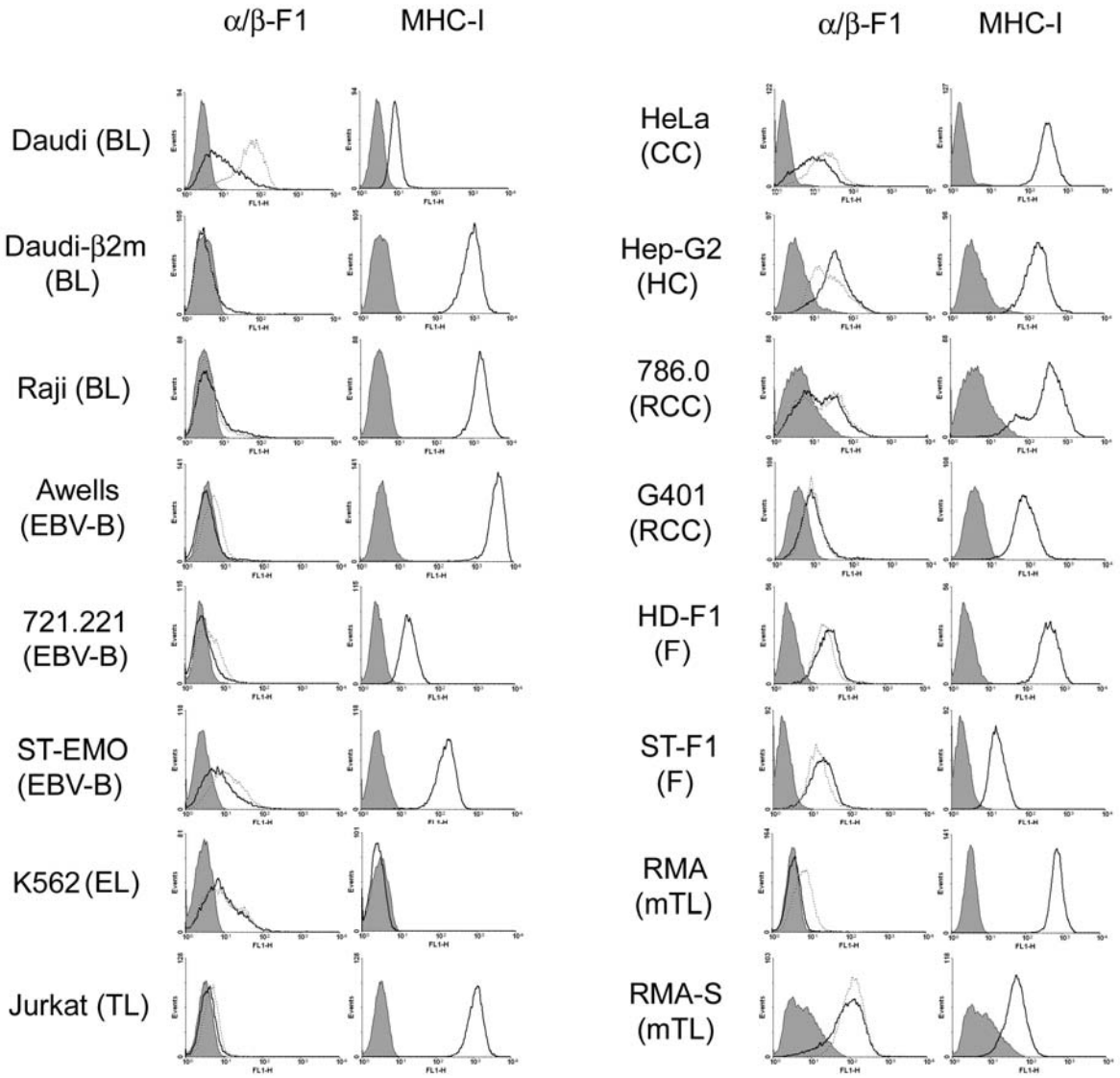

Figure 1: MHC-I and ecto-F_1 expression on cell lines.

Cells were analyzed by standard indirect immunofluorescence for MHC-I (W6/32 for human cell lines, anti-H-$2K^bD^b$ for RMA and RMA-S) and ecto-F_1-ATPase expression (α and β chains) after gating on viable cells on the forward scatter/side scatter dot plot. Cell lines are described in the Material and Methods section. BL: Burkitt's lymphomas; EBV-B: Epstein-Barr virus-transformed B lymphoblastoid cell lines; TL: T-cell leukaemia; HC: Hepatocarcinoma; F: Fibroblasts; mTL: murine T cell lymphoma; W6/32 is an antibody against native MHC-I antigens. Solid lines: anti-α-F_1 or W6/32; dashed lines: anti-β-F_1; Shadowed histograms: irrelevant IgG_1 control.

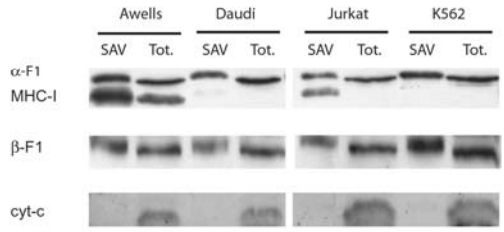

Figure 2: Immunoprecipitation of ecto-F_1 components.

Daudi, Awells, K562 and Jurkat cells were surface-biotinylated. Membrane proteins were precipitated with streptavidin-coated beads and separated by denaturing PAGE. Identical membranes were immunoblotted with anti-α-F_1 and HC10 (anti-MHC-I free heavy chains) antibodies or with anti-β-F_1 and anti-cytochrome c antibodies. Note that ~100 times more cells are used for streptavidin pull-downs than for total lysates (used as size controls for F_1 components). This explains why MHC bands are not detected in total lysates from Jurkat cells. Slight shifts in migration are due to the biotinylation of the surface proteins in streptavidin pull-downs.

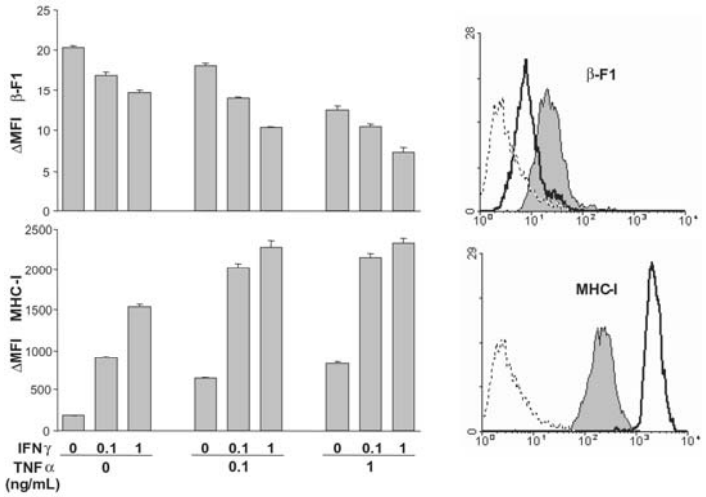

Figure 3: Induction of MHC-class I antigens by cytokine treatment.

A, B: Normal primary fibroblasts were grown for 48 hours in the presence of the indicated concentration of IFN-γ and/or TNF-α to induce the expression of MHC-class I antigens in a dose-dependent fashion. At the end of the culture, cells were recovered and analyzed by flow cytometry for (A) the expression of β-F_1 and (B) MHC-class I antigens (W6/32) as described in Fig.1 and in the Material and Methods section. ΔMFI: mean fluorescence intensity after subtraction of isotype control fluorescence (3.53 +/- 0.45). Each bar is the mean result from triplicate cultures (+/- S.E.M). C: representative histograms of fibroblast staining with anti-βF_1 (top) and W6/32 (bottom) antibodies after culture with IFN-γ and TNF-α (both 1ng/ml; shaded histograms) or control cultures (solid lines). Dashed lines represent the isotype control staining. Similar results were obtained with the HepG2 cell line.

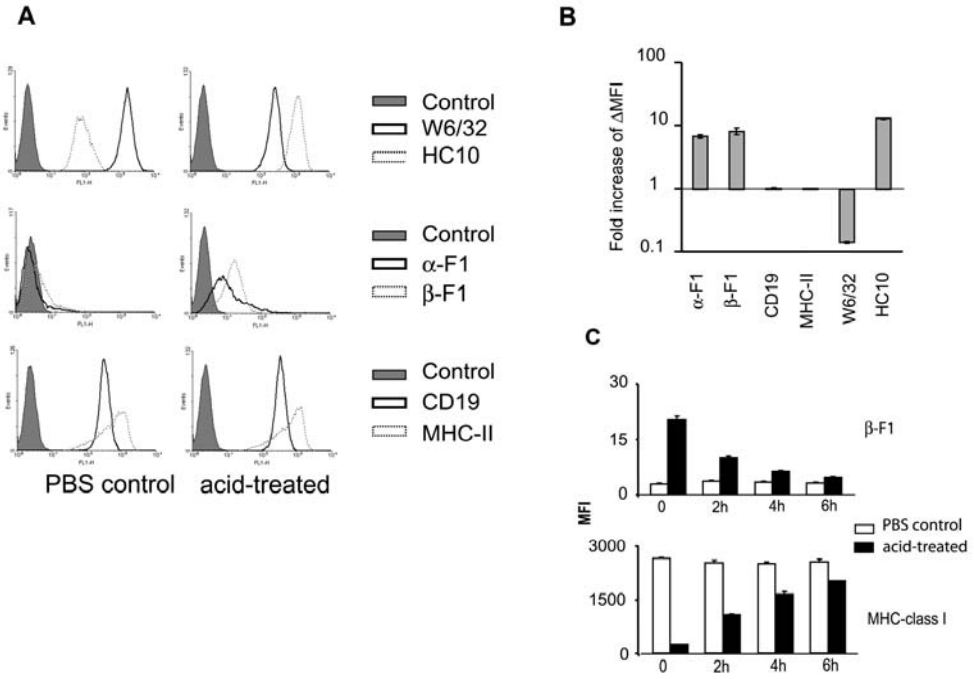

Figure 4: Disruption of surface MHC-class I by acid treatment reveals F_1 components.

A: Raji cells were submitted to brief acid treatment (1min, pH3) and stained for α-F_1, β-F_1, MHC-I and control antigens. CD19: B-cell marker; MHC-II: MHC-class II antigens. W6/32 recognizes native MHC-class I antigens. HC10 is specific for β2-microglobulin-free MHC-class I heavy chains.

B: Quantitative analysis of surface markers on acid-treated Raji cells. Results are expressed as fold increase of the specific fluorescence ΔMFI. ΔMFI = mean fluorescence intensity (MFI) after subtraction of isotype control fluorescence (mean of triplicate similarly-treated cell samples +/- S.E.M.). C: Acid-treated cells or control (PBS-treated) Raji cells were put back in culture and monitored for β-F_1 and MHC-class I expression at the indicated time (mean of triplicate culture experiments +/- S.E.M).

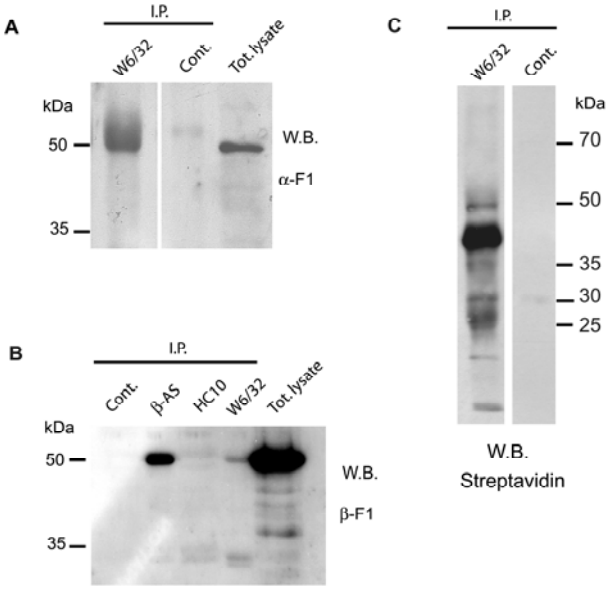

Figure 5: Co-immunoprecipitation of MHC-class I and F_1 subunits.

Raji cells were surface-biotinyated, lysed, and solubilized proteins were immunoprecipitated with the antibody indicated on top of each lane. Immunoprecipitated proteins ($2x10^7$ cells) and total lysates ($2x10^5$ cells) were separated on a 12% poly-acrylamide gel, transferred to nitrocellulose and blotted with anti-α-F_1 (A), anti-β-F_1 (B) or with streptavidin (C) to detect MHC-I-associated membrane proteins. The antibodies used for immunoprecipitations and immunoblotting are described in the Material and Methods section. Note that β-F_1 components (B) are present in W6/32 precipitates (native MHC-I antigens) but not in HC10 precipitates (free MHC-I heavy chains).

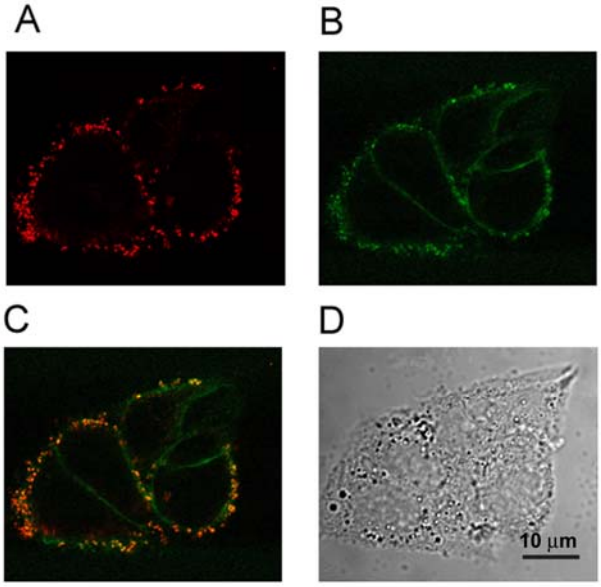

Figure 6: Confocal analysis of MHC-I and β-F_1 on the membrane of HepG2 cells.

Non-permeabilized HepG2 cells were stained simultaneously for native MHC-class I antigens (A; red) and β-F_1 (B; green) as described in the Material and Methods section. Panel C shows the merge of green and red images so that structures which co-localize appear yellow. D: differential interference contrast (DIC) image. Control experiments (not shown) were perfomed to control the isotype specificity of secondary antibody used (see Material and Methods).